Polymer Chemistry

Accepted Manuscript

This is an *Accepted Manuscript*, which has been through the Royal Society of Chemistry peer review process and has been accepted for publication.

Accepted Manuscripts are published online shortly after acceptance, before technical editing, formatting and proof reading. Using this free service, authors can make their results available to the community, in citable form, before we publish the edited article. We will replace this *Accepted Manuscript* with the edited and formatted *Advance Article* as soon as it is available.

You can find more information about *Accepted Manuscripts* in the Information for Authors.

Please note that technical editing may introduce minor changes to the text and/or graphics, which may alter content. The journal's standard Terms & Conditions and the Ethical guidelines still apply. In no event shall the Royal Society of Chemistry be held responsible for any errors or omissions in this *Accepted Manuscript* or any consequences arising from the use of any information it contains.

ROYAL SOCIETY OF CHEMISTRY

www.rsc.org/polymers

Journal Name

ARTICLE

Tuning Optoelectronic Properties of Dual-Acceptor Based Low-Bandgap Ambipolar Polymers by Thiophene-Bridge Length

Received 00th January 20xx,
Accepted 00th January 20xx

DOI: 10.1039/x0xx00000x

www.rsc.org/

Cunbin An,[a‡] Tomasz Marszalek,[a‡] Xin Guo,*[ab] Sreenivasa Reddy Puniredd,[a] Manfred Wagner,[a] Wojciech Pisula[ac] and Martin Baumgarten*[a]

Three very-low-bandgap dual-acceptor based polymers containing diketopyrrolopyrrole (**DPP**) and a thiadiazoloquinoxaline (**TQ**) derivative were prepared. Both acceptors in these polymers were separated by one, two and three thiophenes. Only inserting one thiophene between **DPP** and benzodithiophene condensed **TQ**, polymer **PDPP-T-TQ** has a very low optical bandgap of 0.60 eV with the electron affinity of -4.23 eV. Optical and electrochemical bandgaps of the polymers were enlarged with increasing the thiophene-bridge length between both acceptors. GIWAXS measurements confirmed that polymer with three thiophene bridges (**PDPP-3T-TQ**) showed an ordered arrangement of the crystallites, providing a best ambipolar device performance among these polymers.

Introduction

Conjugated polymers with a very low bandgap (≤ 1.0 eV) have been drawing substantial attention due to their broad and near-infrared (NIR) absorption, multiple redox states in a small potential window, ambipolar charge carrier transport, and potential use in sensors, batteries, and supercapacitors.[1] As a significant breakthrough work, Wudl and his coworkers reported a poly(isothianapthene) with an energy bandgap of ~1.0 eV due to a strong quinoidal character in the thiophene ring.[2-4] Recently, tailoring donor-acceptor (D-A) interactions in D-A copolymers has proven to be an effective strategy for developing very low bandgap polymers. The combination of strong donors and acceptors with quinoidal character has produced soluble polymers with optical bandgaps (E_g^{opt}) lower than 0.70 eV, such as **P(DTP-BThBTT)**[5] and **P(CPDT-TQ)**[6] (Figure 1).

However, many low bandgap polymers containing one strong acceptor carry more holes than electrons, such as those derived from benzobisthiadiazole (**BBT**)[7,8] and diketopyrrolopyrrole (**DPP**)[9,10]. Balanced charge carrier transporting polymers are highly desirable for ambipolar OFETs, which allows both p-type and n-type channels to be realized in one device with simple fabrication processes.[11] For this purpose, a dual-acceptor design strategy has been proposed to construct D-A1-D-A2 polymers.[12-17] For example, **PDPP-BBT** (Figure 1) exhibited an E_g^{opt} of around 0.65 eV and ambipolar charge transporting behavior with mobilities of 1.17 $cm^2 V^{-1} s^{-1}$ for holes and 1.32 $cm^2 V^{-1} s^{-1}$ for electrons.[18] In comparison to the polymers composed of only one strong acceptor, dual-acceptor polymers with very low bandgap and balanced charge carrier transport are rarely studied.

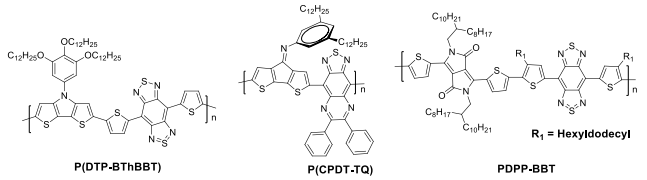

Figure 1. Reported polymers with the very low bandgap (≤ 1.0 eV).

In this paper, we report the combination of two high electron affinity acceptors, **DPP** and benzodithiophene condensed **TQ** in one polymer backbone. As previously demonstrated, this condensed **TQ** was a new strong acceptor and a corresponding D-A copolymer exhibited a very low E_g^{opt} of 0.76 eV and hole-dominant ambipolar behavior.[19,20] On the other hand, **DPP** has been widely studied as a strong acceptor in low bandgap polymers because numerous **DPP**-based polymers have revealed excellent performance as ambipolar semiconductors.[10,21] Therefore, it can be expected that the combination of the two highlighted acceptors could endow the resulting dual-acceptor polymers desired characteristics of both the very low bandgap and the balanced ambipolarity. Three copolymers (**PDPP-T-TQ**, **PDPP-2T-TQ** and **PDPP-3T-TQ** in Scheme 1) were designed and synthesized, in which the two acceptors are separated in the polymer backbone by oligothiophene bridges with varying lengths in order to elaborately tune the optoelectronic properties and charge carrier transport.

Results and Discussion

Synthesis and Characterization

The synthesis of the three polymers is outlined in Scheme 1. In order to introduce different oligothiophenes between **DPP** and condensed **TQ**, three **TQ** monomers (**3**, **4** and **7**) were synthesized by flanking thiophenes onto condensed **TQ** at both sides. Monomer **3** was synthesized from **1** and **2** via a condensation

[a]Max Planck Institute for Polymer Research, Ackermannweg 10, D-55128, Mainz, Germany.
[b]Dalian National Laboratory for Clean Energy, Dalian Institute of Chemical Physics, Chinese Academy of Sciences, 457 Zhongshan Road, Dalian 116023, China.
[c]Department of Molecular Physics, Faculty of Chemistry, Lodz University of Technology, Zeromskiego 116, 90-924 Lodz, Poland.
E-mail: guoxin@dicp.ac.cn; martin.baumgarten@mpip-mainz.mpg.de
‡These authors contributed equally.
Electronic Supplementary Information (ESI) available: Experimental part, CV, TGA, DFT calculation, NMR and HRMS spectra. See DOI: 10.1039/b000000x/

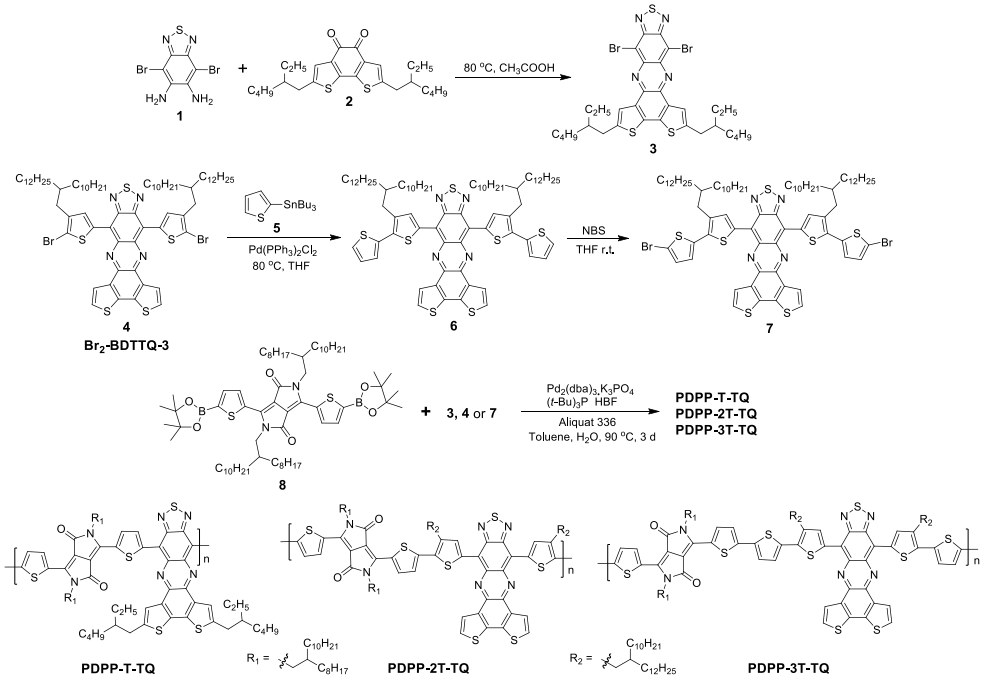

Scheme 1. Synthetic routes for the three polymers.

reaction. Monomer **7** was prepared from **Br_2-BDTTQ-3** after two-step reactions, Stille coupling and bromination. The Suzuki coupling reaction was carried out between monomer **3**, **4** or **7**, and DPP-diboronic ester **(8)** to give corresponding **PDPP-T-TQ**, **PDPP-2T-TQ**, and **PDPP-3T-TQ**, respectively. In previous works,[11,22] when using $Pd_2(dba)_3$ as catalyst tri-tert-butylphosphoniumtetrafluoborate ((*t*-Bu)$_3$P·HBF$_4$) was usually used as an effective ligand to yield high-molecular-weight polymers in Suzuki coupling based on compound **8**. Therefore, the $Pd_2(dba)_3$/(*t*-Bu)$_3$P·HBF$_4$ catalyst system was also chosen here. The number-average molecular weight (M_n) and polydispersity index (PDI) of the three polymers were determined by gel permeation chromatography (GPC) method using polystyrene as standard and tetrahydrofuran as eluent at 30 °C. The data are listed in Table 1. The low M_n of **PDPP-T-TQ** and **PDPP-2T-TQ** might arise from the low reaction activity and the steric hindrance in monomers **3** and **4** preventing producing higher M_n during polymerization. Similar low M_n was also reported for **PDPP-BBT** (Figure 1).[18] Another ligand, tri(*o*-tolyl)phosphine (P(*o*-tol)$_3$) was also attempted to prepare **PDPP-T-TQ** as it was reported that polymers with M_n higher than 10 kg mol^{-1} could be produced when using the $Pd_2(dba)_3$/P(*o*-tol)$_3$ catalyst system in Suzuki coupling based on DPP-diboronic ester.[23-25] The M_n of resulting polymer (6.3 Kg mol^{-1}, PDI: 2.9) is however slightly lower in comparison with that using the ligand of (*t*-Bu)$_3$P·HBF$_4$. After introducing one more electron-rich thiophene onto monomer **4** at both sides, the steric hindrance between **DPP** and monomer **7** was reduced so that the **PDPP-3T-TQ** possessed a higher M_n than the other two polymers. It is thus believed that the sterics around the coupling units play a main role in the limited activity for polymerizations of **PDPP-T-TQ** and **PDPP-2T-TQ.** The three polymers exhibited excellent solubility in common organic solvents such as chloroform and tetrahydrofuran at room temperature. Additionally, the decomposition temperature was measured by thermogravimetric analysis (TGA) (Figure S1) showing 5% weight loss at 380 °C for **PDPP-T-TQ** and **PDPP-2T-TQ**, and 390 °C for **PDPP-3T-TQ**.

Optical and Electrochemical Properties

UV-vis-NIR absorption spectra of the polymers were recorded in chloroform solution (c = 10^{-5} M) as well as in thin films. The relevant data are summarized in Table 1. In dilute chloroform solution, all polymers exhibit three absorption bands as shown in Figure 2a. The first intense band between 300 and 500 nm contains double peaks that are typical for many **TQ** polymers,[26-30] suggesting that this band

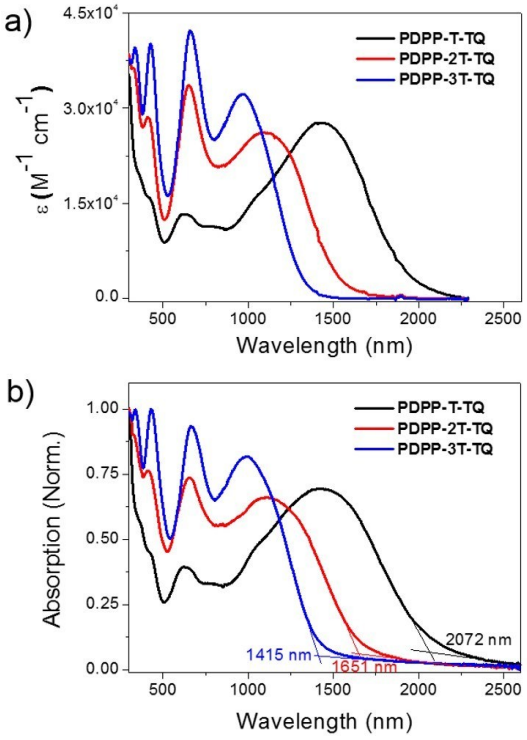

Figure 2. UV-visible-NIR absorption spectra of three polymers (a) in chloroform solutions and (b) in films.

could be contributed by the condensed **TQ** moiety. The second one ranges from 500 to 800 nm, similar to the maximum absorption (λ_{max}) of some **DPP** polymers,[31,32] indicating its origin from the interaction between **DPP** and adjacent thiophene units. The last band broadly covers from 800 to 2250 nm, which is attributed to the intramolecular charge transfer (ICT) between donors and acceptors in the polymer main chains.[33] **PDPP-T-TQ** exhibits inconspicuous **TQ** and **DPP** absorption characters but has a λ_{max} up to 1343 nm, indicating a very strong ICT process within this polymer. Increasing the thiophene bridge to two units between the **DPP** and condensed **TQ** leads to a blue shift of 324 nm at λ_{max} for **PDPP-2T-TQ**. Meanwhile, the absorption profile is much more dominated by the condensed **TQ** and **DPP** moieties. After introducing another thiophene between **DPP** and condensed **TQ** the λ_{max} of **PDPP-3T-TQ** further hypsochromically shifts to 970 nm and more remarkable absorption features of condensed **TQ** and **DPP** are observed.

Thin films were prepared by drop-casting chloroform solutions of the three polymers onto glass slides. The films display slightly red-shifts of 1, 5 and 25 nm at λ_{max} and broadened absorption bands compared with those in solution (Figure 2b), indicating that the obvious red-shift occurs along with the increased backbone coplanarity of the polymers. The tiny red-shifts of **PDPP-T-TQ** and **PDPP-2T-TQ** can be attributed to the disordered morphology of both polymers induced by bulky side chains which retard the efficient packing of polymer chains in the solid state. The optical bandgaps of **PDPP-T-TQ**, **PDPP-2T-TQ** and **PDPP-3T-TQ** were calculated to be 0.60, 0.75 and 0.88 eV, respectively, according to the onset of solid-state absorption spectra. The variation of bandgaps can be explained by the electronic changes in the HOMO and LUMO levels (See DFT calculations for details below). The value of **PDPP-T-TQ** shows a lowest E_g^{opt} among dual-acceptor polymers reported so far.[12,13,34,35] These results demonstrate that changing the distance between **DPP** and **TQ** acceptors by the oligothiophene bridge length is an effective strategy for tuning the optoelectronic properties of the **DPP**-**TQ** dual-acceptor polymers.

The electrochemical properties of three polymers were determined using cyclic voltammetry (CV) from their drop-cast thin films (Figure 3). The corresponding data are summarized in Table 1. The electron affinities (EAs) and ionization potentials (IPs) of the polymers were calculated from the onset of first reduction and oxidation potentials. The values of EA are -4.23, -4.13 and -4.07 eV for **PDPP-T-TQ**, **PDPP-2T-TQ** and **PDPP-3T-TQ**, respectively, while the corresponding IP values are -5.12, -5.06, and -5.08 eV. Interestingly, the different thiophene numbers can significantly alter the EA values compared to their similar IP values. The **PDPP-T-TQ** had a lowest EA value which is related to its strongest ICT ability, leading to a narrowest HOMO-LUMO bandgap among these three polymers. The electrochemical bandgaps of three polymers were calculated to be 0.89, 0.93, 1.01 eV for **PDPP-T-TQ**, **PDPP-2T-TQ** and **PDPP-3T-TQ**, respectively. It is the same tendency with their optical gaps. The only difference is that the electronic bandgaps are larger than their optical gap, which is attributed to the exciton binding energy of conjugated polymers.[36]

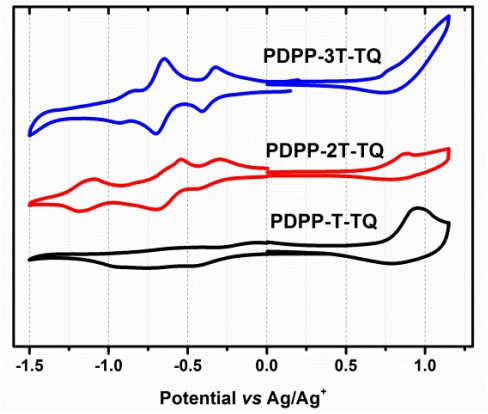

Figure 3. Cyclic voltammograms of **PDPP-T-TQ**, **PDPP-2T-TQ** and **PDPP-3T-TQ** in films.

OFET Properties

Bottom-gate, bottom-contact OFETs were fabricated in order to evaluate the charge transport properties of all three polymers. All polymers were deposited by drop-casting 5 mg/mL chloroform solution on silicon/silicone dioxide (SiO_2) substrates in nitrogen atmosphere, followed by annealing at 150 °C for 1 h. The 300 nm thick SiO_2 dielectric covering the highly doped Si and acting as the gate electrode was functionalized with hexamethyldisilazane (HMDS) to minimize interfacial trapping sites. Representative transfer and output characteristics of **PDPP-3T-TQ** are shown in Figure 4. Such curves of other two polymers are presented in the Figure S2 (Supporting Information). All polymers show ambipolar device behaviors. In all cases the charge carrier mobilities are calculated from the drain current saturation region. Polymer **PDPP-T-TQ** exhibits balanced charge transport with hole and electron mobilities of 2×10^{-5} cm^2 V^{-1} s^{-1} and 3×10^{-5} cm^2 V^{-1} s^{-1}. Additional thiophene units in the bridge between the **DPP** and **TQ** acceptor units (**PDPP-2T-TQ**) in comparison to **PDPP-T-TQ** do not change the charge carrier mobilities with 4×10^{-5} cm^2 V^{-1} s^{-1} for electrons and 1×10^{-5} cm^2 V^{-1} s^{-1} for holes. But a difference in transport behavior is observed for **PDPP-3T-TQ**, which exhibits a hole mobility of 5×10^{-4} cm^2 V^{-1} s^{-1} being one order of magnitude higher than for **PDPP-T-TQ** and **PDPP-2T-TQ**. These results implied that the thiophene bridge length between **DPP** and condensed **TQ** can transform the **DPP-TQ** based polymers from well-balanced ambipolar to hole-dominant ambipolar behavior. However, for all polymers a contact resistance is observed in the transfer and output curves.

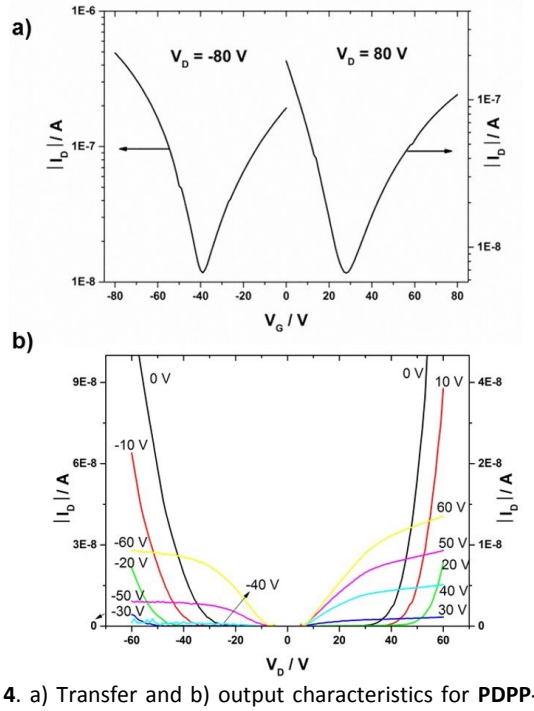

Figure 4. a) Transfer and b) output characteristics for **PDPP-3T-TQ** thin films.

Table 1. Molecular weights, decomposition temperatures, optical absorptions, electrochemical properties and field-effect mobilities of **PDPP-T-TQ**, **PDPP-2T-TQ** and **PDPP-3T-TQ**.

Polymer	M_w/M_n (kg/mol)[a]	T_d (°C)[b]	λ_{abs} (nm) soln.[c]	λ_{abs}(nm) film[d]	E_g^{opt} (eV)[d]	IP (eV)[e]	EA (eV)[e]	μ_h ($cm^2\ V^{-1}\ s^{-1}$)[f]	μ_e ($cm^2\ V^{-1}\ s^{-1}$)[f]
PDPP-T-TQ	26.3/7.4	380	1434	1435	0.60	-5.12	-4.23	2×10^{-5}	3×10^{-5}
PDPP-2T-TQ	23.1/7.3	380	1110	1115	0.75	-5.06	-4.13	1×10^{-5}	4×10^{-5}
PDPP-3T-TQ	43.9/13.2	390	970	995	0.88	-5.08	-4.07	5×10^{-4}	5×10^{-5}

[a]Determined by GPC in THF using polystyrene standards; [b]Temperature of decomposition corresponding to 5% weight loss from TGA analysis under N_2 with the heating rate of 10 °C/min; [c]Dissolved in chloroform (c = 10^{-5} M); [d]Drop-cast from chloroform solution (2 mg/mL); [e]IP and EA were estimated from the onsets of the first oxidation and reduction peak, while the potentials were determined using ferrocene (Fc) as standard by empirical formulas IP/EA = -($E_{Ox/Red}^{onset}$- $E_{Fc/Fc+}^{1/2}$+4.8) eV, wherein $E_{Fc/Fc+}^{1/2}$ = 0.40 eV. [f]Average value out of 10 devices.

Self-Organization in Bulk

In order to understand the supramolecular organization of the polymer films, grazing incident X-ray wide angle scattering (GIWAXS) was carried out. GIWAXS gives valuable information about the surface organization of the polymers in thin films.[37] For these measurements the same procedure for the film preparation was used as that for the transistor devices. Figure 5 presents the GIWAXS patterns of the three polymers which reveal slight variations between **PDPP-T-TQ** and **PDPP-2T-TQ**. For both polymers an interlayer distance of 1.60 nm and 2.17 nm is determined from the position of the main reflection in small-angle range. The larger interlayer spacing for **PDPP-2T-TQ** is directly related to longer side chains. The isotropic distribution of these reflections suggests a lack of long-range order and a random arrangement of the crystallites towards the surface. A characteristic π-stacking reflection is missing indicating a disordered organization of the polymer chains within the layer structures.

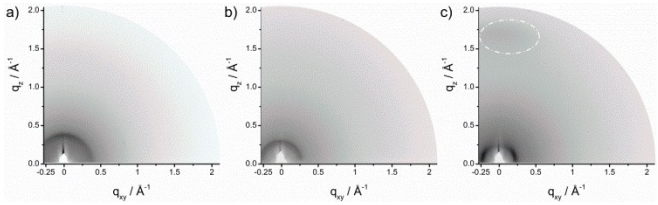

Figure 5. GIWAXS patterns of a) **PDPP-T-TQ**, b) **PDPP-2T-TQ** and c) **PDPP-3T-TQ** thin films. Reflections corresponding to π-stacking are indicated by dashed circles.

In contrast, the GIWAXS pattern of **PDPP-3T-TQ** (Figure 5c) exhibits more distinct reflections. In the small-angle region, the maximum intensity of the reflection is located on the equatorial plane of the pattern, whereby an interlayer distance of 2.65 nm is found. This reflection position in the pattern is indicative for a face-on orientation of the polymer on the surface. This conclusion is verified by the appearance of a π-stacking scattering intensity (Figure S3) on the meridional plane at q_z = 1.7 Å^{-1} (0.36 nm). The π-stacking reflection implied a better order arrangement of thin films for **PDPP-3T-TQ** in comparison to the other two polymers. Increasing the number of the thiophene moieties changes the linearity and planarity of the conjugated polymer backbones and reduces the twist between **DPP** and **TQ** groups improving the polymer packing. Additionally, the face-on arrangement allows a 3D transport in the active layer.[38] This is the main reason for the higher charge carrier mobility of **PDPP-3T-TQ**. However, it could not provide an explanation why increasing the thiophene bridge length changes the transistor characteristics from well-balanced ambipolar to hole-dominant ambipolar behavior. Therefore, density functional theory (DFT) calculations were carried out.

Density Functional Theory Calculations

DFT calculations were carried out on monomeric unit of the polymers, named **DPP-T-TQ**, **DPP-2T-TQ** and **DPP-3T-TQ**, carrying methyl substituents. The distribution of electron was simulated by density functional theory (DFT) using the Gaussian 03 program[39] with B3LYP functional and 6-31G basis set.[40] The electron density distributions of the LUMO and HOMO of geometry with optimized structures are shown in Figure 6. All HOMO levels of three monomeric units were very similar with delocalization along the conjugated backbone. However, the electron density became gradually localization on **TQ** segment in the LUMO levels as the increased thiophene bridge length. Such electron density distribution on the HOMO and LUMO level forces an unbalanced transport along conjugated backbone in the case of **DPP-3T-TQ**. This tendency is quite obvious for the hole transport which increases with increasing the number of thiophene units while the electron transport remains constant. In addition, the results from calculations were well consistent with the observations from CV results, demonstrating the thiophene bridge length can significantly alter the EA in comparison with IP. It can hence be concluded that the thiophene bridge length not only tune the organization behavior in thin films but also can strongly influence the ratio of electron and hole carrier mobilities.

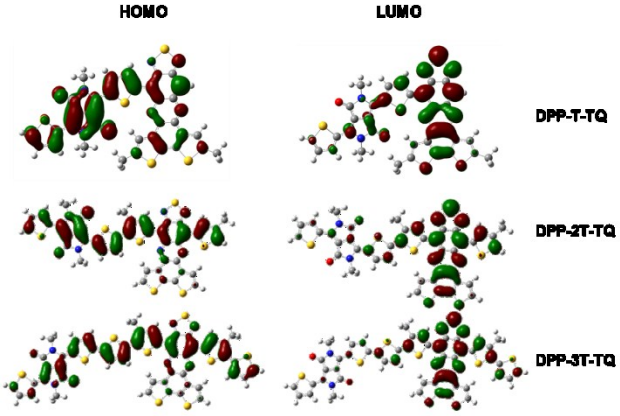

Figure 6. The electron density distribution on one repeat unit of **PDPP-T-TQ, PDPP-2T-TQ** and **PDPP-3T-TQ**.

Conclusions

We have successfully synthesized three D-A1-D-A2 dual-acceptor polymers. The both acceptors in these polymers were separated by thiophene bridges with different length. Polymer **PDPP-T-TQ** possessed a very narrow optical bandgap of 0.60 eV. The E_g^{opt} of polymers are significantly increased from 0.60 to 0.88 eV with increased thiophene bridge length between both acceptors. The CV measurement indicated high electron affinities of the polymers ranging from -4.07 to -4.23 eV. From polymers **PDDP-2T-TQ** to **PDPP-3T-TQ**, although the intramolecular charge transfer abilities of polymers were decreased, the planarity of polymer was improved as confirmed by GIWAXS. **PDPP-3T-TQ** exhibited a hole-dominant ambipolar behavior with 5×10^{-4} cm^2 V^{-1} s^{-1} for holes and 5×10^{-5} cm^2 V^{-1} s^{-1} for electrons; the hole mobility was one order of magnitude higher than **PDPP-2T-TQ.** The correlations between structures and charge carrier mobilities of **DPP-TQ** copolymers are beneficial to broaden the understanding of optoelectronic properties of such polymers and to further design new dual-acceptor polymers towards well balanced ambipolarity.

Experimental Section

General methods

^1H NMR and ^{13}C NMR spectra were recorded in deuterated solvents on a Bruker DPX 250. ^1H NMR of the polymers spectra were recorded in $C_2D_2Cl_4$ solvents on Bruker DPX 500 at 373K. High Resolution Mass Spectra (HRMS) were carried out by the Microanalytical Laboratory of Johannes Gutenberg-University, Mainz. Elemental analysis was carried out using a Foss Heraeus Vario EL in the Institute of Organic Chemistry at the Johannes Gutenberg-University, Mainz. UV–Vis-NIR absorption spectra were measured on a Perkin-Elmer Lambda 9 spectrophotometer at room temperature. Thermogravimetry analysis (TGA) was carried out on a Mettler 500 Thermogravimetry Analyzer. Cyclic Volatammetry (CV) was carried out on a computer-controlled GSTAT12 in a three-electrode cell in anhydrous Acetonitrile solvents solution of Bu_4NPF_6 (0.1 M) with a scan rate of 50 mV/s at room temperature under argon. A Pt wire, a silver wire, and a glassy carbon electrode were used as the counter electrode, the reference electrode, and the working electrode, respectively. The molecular weights were determined by PSS-WinGPC (PSS) (pump: alliance GPC 2000) GPC equipped with an UV or RI detector running in THF at 30 °C using a PLgel MIXED-B column (particle size: 10 mm, dimension: 0.8×30 cm) calibrated against polystyrene standards.

OFET device fabrication and measurements

All FETs were fabricated employing the bottom-gate, bottom-contact architecture. The 230 nm thick SiO_2 dielectric covering the highly doped Si acting as the gate electrode was functionalized with hexamethyldisilazane (HMDS) to minimize interfacial trapping sites. Polymer thin films were deposited by drop-casting 5 mg/mL chloroform solution on FET substrates in nitrogen atmosphere, followed by annealing at 150 °C for 1 h. The channel lengths and widths are 20 and 1400 mm, respectively. All the electrical measurements (using Keithley 4200 SCS) are performed in a glove box under nitrogen atmosphere.

Grazing incidence wide angle X-ray scattering (GIWAXS).

GIWAXS experiments were performed by means of a solid anode X-ray tube (Siemens Kristalloflex X-ray source, copper anode X-ray tube operated at 30 kV and 20 mA). Osmic confocal MaxFlux optics, X-ray beam with pinhole collimation and a MAR345 image plate detector. The samples were prepared as thin film with the same procedure as that used in OFETs fabrication.

Synthetic details

All chemicals and reagents were used as received from commercial sources without further purification unless stated otherwise. Chemical reactions were carried out under ambient atmosphere. The intermediate compounds 4,7-dibromobenzo[c][1,2,5]thiadiazole-5,6-diamine (**1**),[41] 2,7-bis(2-ethylhexyl)benzo[2,1-b:3,4-b']dithiophene-4,5-dione (**2**),[19] **Br_2-BDTTQ-3** (**4**),[20] 3,6-bis-(5-(4,4,5,5-tetramethyl-1,3,2-dioxaborolan-thiophen-2-yl))-N,N-bis(octyldodecyl)-1,4-dioxo-pyrrolo[3,4-c] pyrrole (**8**)[22] were prepared according to published procedures.

8,12-Dibromo-2,5-bis(2-ethylhexyl)-[1,2,5]thiadiazolo[3,4-i]dithieno[3,2-a:2',3'-c]phenazine (3)

A suspension of **1** (0.40 g, 1.23 mmol), **2** (0.55 g, 1.23 mmol) and 35 mL acetic acid were placed into a 50 mL Schlenk tube. The mixture was heated to 80 ºC and stirred overnight. After cooling to room temperature, the product was filtered and washed with methanol, then purified by column chromatography using hexane/dichloromethane (3/1) as eluent to give 0.77 g of compound **3** (dark green solid, 85 %). ^1H NMR (250 MHz, CD_2Cl_2) δ 8.03 (s, 2H), 3.00 (dd, *J* = 2.5 Hz, *J* = 5.0 Hz, 4H), 1.76 (m, 2H), 1.41 (br, 16H), 0.95 (br, 12H). ^{13}C NMR (62.5 MHz, $CDCl_3$) δ 151.65, 145.10, 142.45, 137.39, 137.66, 133.30, 123.47, 113.40, 41.74, 34.87, 32.63, 29.09, 25.76, 23.19, 14.35, 11.03. HRMS (ESI+): m/z calcd 731.0547, found 731.0541.

8,12-Bis(3-(2-decyltetradecyl)-[2,2'-bithiophen]-5-yl)-[1,2,5]thiadiazolo[3,4-i]dithieno[3,2-a:2',3'-c]phenazine (6).

Br_2-BDTTQ-3 (**4**) (0.35g, 0.26 mmol), 2-tributylstanylthiophene **5** (0.30 g, 0.78 mmol) and $Pd(PPh_3)Cl_2$ (21 mg, 0.026 mmol) were dissolved in 15 mL of anhydrous THF under argon. The resulting solution was stirred for 16 h at 80 °C. The solvent was removed under reduced pressure to afford a dark-red oil, which was purified by column chromatography to give 0.29 g (dark-green solid, 82%) of compound **6**. ^1H NMR (250 MHz, CD_2Cl_2, ppm) δ 8.62 (s, 2H), 7.79 (d, *J* = 5.0 Hz, 2H), 7.33 (t, *J* = 5.0 Hz, *J* = 2.5 Hz, 2H), 7.08 (m, 6H), 2.67 (d, *J* = 7.50 Hz, 4H), 1.80 (m, 2H), 1.38-1.23 (m, 80H), 0.89-0.84 (m, 12H). ^{13}C NMR (62.5 MHz, CD_2Cl_2, ppm) δ 150.67, 138.82, 137.89, 137.85, 137.77, 137.72, 137.04, 134.68, 134.45, 134.35, 127.92, 126.88, 125.29, 125.13, 124.40, 119.14, 38.77, 34.43, 33.77, 32.40, 32.37, 30.76, 30.32, 30.28, 30.25, 30.20, 30.15, 29.87, 29.83, 26.82, 23.13, 14.33. HRMS (ESI+): m/z calc. 1351.6854, found 1351.6850.

8,12-Bis(5'-bromo-3-(2-decyltetradecyl)-[2,2'-bithiophen]-5-yl)-[1,2,5]thiadiazolo[3,4-i]dithieno[3,2-a:2',3'-c]phenazine (7)

Compound **6** (0.25 g, 0.18 mmol) was dissolved in 15 mL of THF at room temperature. NBS (72.4 mg, 0.41 mmol) was carefully added into the solution in small batches under dark. The mixture was stirred for 5 h. After removing the solvent under reduced pressure, the residue was purified by column chromatography to give monomer **7** as a dark-green solid (0.24 g, 86 %). ^1H NMR (250

MHz, CD_2Cl_2) ^{1}H NMR (250 MHz, THF-d_8, ppm) δ 8.66 (s, 2H), 7.93 (d, *J* = 5.0 Hz, 2H), 7.38 (d, *J* = 5.0 Hz, 2H), 7.11 (d, *J* = 2.5 Hz, 2H), 6.92 (d, *J* = 5.0 Hz, 2H), 2.67 (d, *J* = 7.50 Hz, 4H), 1.81 (br, 2H), 1.39-1.22 (m, 80H), 0.88-0.83 (m, 12H). ^{13}C NMR (62.5 MHz, THF-d_8, ppm) δ 150.97, 139.75, 139.48, 138.51, 138.13, 138.10, 137.79, 137.27, 135.12, 134.94, 131.38, 127.24, 126.00, 125.44, 119.47, 112.10, 39.21, 34.84, 34.22, 32.76, 32.73, 31.11, 30.67, 30.62, 30.57, 30.51, 30.24, 30.19, 27.26 (overlap by THF-d_8) 23.41, 14.33. HRMS (ESI+): m/z calcd 1507.5063, found 1507.5059.

Synthesis of PDPP-T-TQ

To a solution of compounds **3** (0.05 mmol) and **8** (0.05 mmol), tri-tert butylphosphoniumtetrafluoborate ((*t*-Bu)$_3$P·HBF$_4$, 0.0067 mmol), tris(dibenzylideneacetone)dipalladium(0) ($Pd_2(dba)_3$), 0.00335 mmol) and aliquat 336 (2 drops) in 6 mL of toluene was added a solution of potassium phosphate (0.074 g, 0.35 mmol) in 0.46 mL of degassed water. The mixture was vigorously stirred at 90 ° C for 3 days. The polymer was end-capped with phenyl units by adding phenyl boronic acid and bromobenzene in sequence. After cooling to room temperature, the reaction mixture was poured into vigorously stirred methanol (100 mL). The polymer was filtered and subjected to Soxhlet extraction with methanol, acetone and hexane. The hexane fraction was collected and added 30 mL of sodium diethyldithiocarbamate aqueous solution (1g/100 ml) to remove residual palladium catalyst, the mixture was heated to 60 °C with vigorous stirring for 2 h. The mixture was separated and organic phase was washed with water for 3 times. The hexane solution was concentrated and precipitated in methanol. The resulting solid was collected by filtration and dried in vacuum to afford black solid (55 mg, 77 %). Molecular weight by GPC (30 °C): M_n = 7.4 kDa, PDI = 3.54. UV-Vis: λ_{max} (solution in chloroform): 1434 nm, 616 nm, 415 nm and 350 nm; λ_{max} (thin film): 1435 nm, 624 nm and 424 nm. The ^{1}H NMR spectra is presented in Figure S9. Elemental analysis: Calcd. for $C_{86}H_{122}N_6O_2S_5$: C 72.12, H 8.59, N 5.87, S 11.19; found: C 72.00, H 8.82, N 5.92, S 10.92.

Synthesis of PDPP-2T-TQ and **PDPP-3T-TQ**

These two polymers were prepared using monomers **4** and **7** instead of monomer **3** in similar procedure and work-up to **PDPP-T-TQ**.

PDPP-2T-TQ (black solid, 75 mg, 74 %). Molecular weight by GPC (30 °C): M_n = 7.3 kDa, PDI = 3.18. UV-Vis: λ_{max} (solution in chloroform): 1110 nm, 655 nm, 418 nm and 328 nm; λ_{max} (thin film): 1115 nm, 656 nm, 418 nm and 332 nm. The ^{1}H NMR spectra is presented in Figure S10. Elemental analysis: Calcd. for $C_{126}H_{190}N_6O_2S_7$: C 73.99, H 9.36, N 4.11, S 10.97; found: C 73.60, H 9.65, N 3.99, S 10.92.

PDPP-3T-TQ (black solid, 88 mg, 80 %). Molecular weight by GPC (30 °C): M_n = 13.2 kDa, PDI = 3.31. UV-Vis: λ_{max} (solution in chloroform): 971 nm, 661 nm, 430 nm and 334nm; λ_{max} (thin film): 995 nm, 664 nm, 418 nm and 339 nm. The ^{1}H NMR spectra is presented in Figure S11. Elemental analysis: Calcd. for $C_{134}H_{194}N_6O_2S_9$: C 73.84, H 8.85, N 3.80, S 13.06; found: C 72.55, H 9.15, N 3.73, S 12.88.

Acknowledgements

This work is supported by SFB-TR49. C.A. gratefully acknowledges the China Scholarship Council (CSC) for offering a 3 years Scholarship.

Notes and references

1 T. A. Skotheim and J. R. Reynolds *Handbook of conducting polymers, Third ed.; Conjugated Polymers: Theory, Synthesis, Properties, and Characterization*, CRC press LLC: Boca Raton, FL, 2007.
2 F. Wudl, M. Kobayashi and A. J. Heeger, *J. Org. Chem.*, 1984, **49**, 3382-3384.
3 J. L. Brédas, A. J. Heeger and F. Wudl, *J. Chem. Phys.*, 1986, **85**, 4673-4678.
4 I. Hoogmartens, P. Adriaensens, D. Vanderzande, J. Gelan, C. Quattrocchi, R. Lazzaroni and J. L. Bredas, *Macromolecules*, 1992, **25**, 7347-7356.
5 T. T. Steckler, X. Zhang, J. Hwang, R. Honeyager, S. Ohira, X.-H. Zhang, A. Grant, S. Ellinger, S. A. Odom, D. Sweat, D. B. Tanner, A. G. Rinzler, S. Barlow, J.-L. Brédas, B. Kippelen, S. R. Marder and J. R. Reynolds, *J. Am. Chem. Soc.*, 2009, **131**, 2824-2826.
6 M. E. Foster, B. A. Zhang, D. Murtagh, Y. Liu, M. Y. Sfeir, B. M. Wong and J. D. Azoulay, *Macromol. Rapid Commun.*, 2014, **35**, 1516-1521.
7 J. D. Yuen, R. Kumar, D. Zakhidov, J. Seifter, B. Lim, A. J. Heeger and F. Wudl, *Adv. Mater.*, 2011, **23**, 3780-3785.
8 J. Fan, J. D. Yuen, M. F. Wang, J. Seifter, J. H. Seo, A. R. Mohebbi, D. Zakhidov, A. Heeger and F. Wudl, *Adv. Mater.*, 2012, **24**, 2186-2190.
9 L. Bürgi, M. Turbiez, R. Pfeiffer, F. Bienewald, H.-J. Kirner and C. Winnewisser, *Adv. Mater.*, 2008, **20**, 2217-2224.
10 Z. Y. Chen, M. J. Lee, R. S. Ashraf, Y. Gu, S. Albert-Seifried, M. M. Nielsen, B. Schroeder, T. D. Anthopoulos, M. Heeney, I. McCulloch and H. Sirringhaus, *Adv. Mater.*, 2012, **24**, 647-652.
11 X. Guo, S. R. Puniredd, B. He, T. Marszalek, M. Baumgarten, W. Pisula and K. Müllen, *Chem. Mater.*, 2014, **26**, 3595-3598.
12 P. Sonar, S. P. Singh, Y. Li, M. S. Soh and A. Dodabalapur, *Adv. Mater.*, 2010, **22**, 5409-5413.
13 S. Cho, J. Lee, M. Tong, J. H. Seo and C. Yang, *Adv. Funct. Mater.*, 2011, **21**, 1910-1916.
14 R. S. Ashraf, A. J. Kronemeijer, D. I. James, H. Sirringhaus and I. McCulloch, *Chem. Commun.*, 2012, **48**, 3939-3941.
15 P. Sonar, T. R. B. Foong, S. P. Singh, Y. N. Li and A. Dodabalapur, *Chem. Commun.*, 2012, **48**, 8383-8385.
16 A. J. Kronemeijer, E. Gili, M. Shahid, J. Rivnay, A. Salleo, M. Heeney and H. Sirringhaus, *Adv. Mater.*, 2012, **24**, 1558-1565.
17 X. Guo, M. Baumgarten and K. Müllen, *Prog. Polym. Sci.*, 2013, **38**, 1832-1908.
18 J. D. Yuen, J. Fan, J. Seifter, B. Lim, R. Hufschmid, A. J. Heeger and F. Wudl, *J. Am. Chem. Soc.*, 2011, **133**, 20799-20807.
19 C. An, S. R. Puniredd, X. Guo, T. Stelzig, Y. Zhao, W. Pisula and M. Baumgarten, *Macromolecules*, 2014, **47**, 979-986.
20 C. An, M. Li, T. Marszalek, D. Li, R. Berger, W. Pisula and M. Baumgarten, *Chem. Mater.*, 2014, **26**, 5923-5929.
21 J. Lee, A. R. Han, H. Yu, T. J. Shin, C. Yang and J. H. Oh, *J. Am. Chem. Soc.*, 2013, **135**, 9540-9547.
22 X. Guo, S. R. Puniredd, M. Baumgarten, W. Pisula and K. Müllen, *Adv. Mater.*, 2013, **25**, 5467-5472.
23 C. Kanimozhi, N. Yaacobi-Gross, K. W. Chou, A. Amassian, T. D. Anthopoulos, and S. Patil, *J. Am. Chem. Soc.*, 2012, **134**, 16532–16535.

24 S. Chen, B. Sun, W. Hong, Z. Yan, H. Aziz, Y. Meng, J. Hollinger, D. S. Seferos and Y. Li, *J. Mater. Chem. C*, 2014, **2**, 1683 –1690.
25 J. Yao, Z. Cai, Z. Liu, C. Yu, H. Luo, Y. Yang, S. Yang, G. Zhang, and D. Zhang, Macromolecules 2015, **48**, 2039−2047.
26 M. Li, C. An, T. Marszalek, X. Guo, Y.-Z. Long, H. Yin, C. Gu, M. Baumgarten, W. Pisula and K. Müllen, *Chem. Mater.*, 2015, **27**, 2218-2223.
27 C. An, M. Li, T. Marszalek, X. Guo, W. Pisula and M. Baumgarten, *J. Mater. Chem. C*, 2015, **3**, 3876-3881.
28 T. L. Dexter Tam, T. Salim, H. Li, F. Zhou, S. G. Mhaisalkar, H. Su, Y. M. Lam and A. C. Grimsdale, *J. Mater. Chem.*, 2012, **22**, 18528-18534.
29 M. L. Keshtov, D. V. Marochkin, V. S. Kochurov, A. R. Khokhlov, E. N. Koukaras and G. D. Sharma, *Poly. Chem.*, 2013, **4**, 4033-4044.
30 T. T. Steckler, P. Henriksson, S. Mollinger, A. Lundin, A. Salleo and M. R. Andersson, *J. Am. Chem. Soc.*, 2014, **136**, 1190-1193.
31 W. Li, W. S. C. Roelofs, M. M. Wienk and R. A. J. Janssen, *J. Am. Chem. Soc.*, 2012, **134**, 13787-13795.
32 S. K. Son, B. S. Kim, C.-Y. Lee, J. S. Lee, J. H. Cho, M. J. Ko, D.-K. Lee, H. Kim, D. H. Choi and K. Kim, *Sol. Energy Mater. Sol. Cells*, 2012, **104**, 185-192.
33 Y. Lee and W. H. Jo, *J. Phys. Chem. C*, 2012, **116**, 8379-8386.
34 G. Zhang, J. Guo, J. Zhang, P. Li, J. Ma, X. Wang, H. Lu and L. Qiu, *Poly. Chem.*, 2015, **6**, 418-425.
35 H.-J. Song, D.-H. Kim, E.-J. Lee, S.-W. Heo, J.-Y. Lee and D.-K. Moon, *Macromolecules*, 2012, **45**, 7815-7822.
36 N. S. Sariciftci, *Primary Photoexcitations in Conjugated Polymers:Molecular Excitons vs Semiconductor Band Model; World Scientific: Singapore, 1997.*
37 J. Rivnay, S. C. B. Mannsfeld, C. E. Miller, A. Salleo and M. F. Toney, *Chem. Rev.*, 2012, **112**, 5488-5519.
38 J. Mei, D. H. Kim, A. L. Ayzner, M. F. Toney and Z. Bao, J. Am. Chem. Soc., 2011, **133**, 20130-20133.
39 Frisch, M. J. et al. Gaussian 03, Revision B.04: Gaussian, Inc., Pittsburgh PA, 2003.
40 A. D. Becke, *J. Chem. Phys.*, 1993, **98**, 5648-5652.
41 H. Li, F. Zhou, T. L. D. Tam, Y. M. Lam, S. G. Mhaisalkar, H. Su and A. C. Grimsdale, *J. Mater. Chem. C*, 2013, **1**, 1745-1752.

TOC

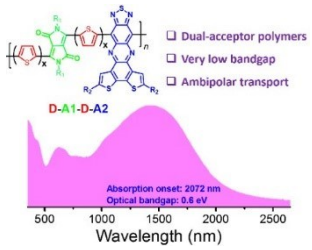

Dual-acceptor polymers based on DPP and TQ are prepared with very low bandgaps (0.6-0.9 eV) and ambipolar charge carrier transports.